Cancer Management and Research

Dovepress

open access to scientific and medical research

Open Access Full Text Article

ORIGINAL RESEARCH

Expression of Carboxypeptidase X M14 Family Member 2 Accelerates the Progression of Hepatocellular Carcinoma via Regulation of the gp130/JAK2/Stat1 Pathway

This article was published in the following Dove Press journal:
Cancer Management and Research

Yanshuo Ye[1]
Yuan An[1]
Min Wang[2]
Hongyu Liu[1]
Lianyue Guan[1]
Zhanpeng Wang[1]
Wei Li[1]

[1]Department of Hepatobiliary-Pancreatic Surgery, China-Japan Union Hospital of Jilin University, Changchun, People's Republic of China; [2]Department of Pathology, Jilin Provincial Cancer Hospital, Changchun 130012, People's Republic of China

Background: Carboxypeptidase X, M14 family member 2 (CPXM2) has been reported to be involved with several human malignancies. However, the impact of CPXM2 on human hepatocellular carcinoma (HCC) tumorigenesis has not been studied.

Materials and Methods: Using immunohistochemistry, the detailed CPXM2 expression patterns were examined in HCC cell lines and tissues. Additionally, a hepatic stellate cell line overexpressing CPXM2 and an HCC CPXM2-knockdown cell line were established by lipofection of an expression plasmid or short hairpin RNA, respectively. The transfection efficiencies were confirmed by reverse transcription-quantitative PCR, Western blotting and immunofluorescence. Moreover, Western blotting was conducted to determine the phosphorylation levels of the tyrosine kinase 2 (JAK2)/signal transducer and activator of transcription 3 (Stat1) pathway. Furthermore, gp130-specific hairpin RNA was used to knockdown gp130 expression in hepatic stellate cells overexpressing CPXM2. The malignant phenotype of cultured HCC cells was assessed by a Cell Counting Kit-8 (CCK8) assay, plate cloning assay, Matrigel invasion assay and wound-healing assay in vitro.

Results: It was demonstrated that CPXM2 was upregulated in HCC, and its upregulation predicted a poor prognosis. Besides, the upregulation of CPXM2 markedly enhanced the metastatic potential of HCC via the gp130/JAK2/Stat1 signaling pathway in vitro.

Conclusion: In summary, this evidence suggests a positive role for CPXM2 in HCC progression via modulation of the gp130/JAK2/Stat1 signaling pathway in HCC.

Keywords: carboxypeptidase XM14 family member 2, hepatocellular carcinoma, metastasis

Introduction

Human hepatocellular carcinoma (HCC) is a common malignance with a poor prognosis and high recurrence rate.[1,2] To date, HCC has a high mortality rates worldwide, and the synthetic therapy of progressive HCC was still unsatisfactory.[3] Hence, it is meaningful to clarify the pathogenesis of HCC tumorigenesis.[4] Previously, carboxypeptidases (CPs) have been validated to play many diverse biological roles by removing C-terminal amino acids from proteins and peptides.[5,6] Genomic disorders in CPs have been revealed to lead to numerous diseases.[7–9] In mammals, the M14 family of CPs, which comprises 25 family members, is the largest family of enzymes that mediates C-terminal residue cleavage.[10,11] Although not all CPs exhibit active peptidase activity, members of

Correspondence: Wei Li
Department of Hepatobiliary-Pancreatic Surgery, China-Japan Union Hospital of Jilin University, Changchun, People's Republic of China
Email weili888@jlu.edu.cn

submit your manuscript | www.dovepress.com
DovePress
http://doi.org/10.2147/CMAR.S228984

the M14 family have various physiological functions on account of their substrate specificity, tissue distribution, and cellular and subcellular localization.[12,13] Carboxypeptidase X (CPX), M14 family member 2 (CPXM2) is a member of the M14 family and has been shown to be associated with several developmental disorders by affecting the cell-cell interactions.[14–17] To date, the impact of CPXM2 on HCC tumorigenesis has not been further explored. Here, CPXM2 expression was found to be overexpressed in HCC tissues, and its overexpression predicted an unfavorable prognosis. Previously, it was demonstrated that glycoprotein 130 (gp130)-mediated signaling can trigger the activation of JAKs and has a vital impact on HCC progression.[18] However, the impact of CPXM2 and its regulatory effect on the gp130/JAK2/Stat1 axis in the tumorigenesis of HCC remain uncertain.

Materials and Methods

Cell Culture and Transfection

The human embryonic kidney cells (293T) cells, the hepatic stellate cell line LX2, and the HCC cell lines (Hep3B, Huh1 and MHCC97H) were obtained from The Cell Bank of Type Culture Collection of the Chinese Academy of Sciences. These cell lines were cultured in DMEM with 10% FBS (Gibco; Thermo Fisher Scientific, Inc.), 100 units/mL penicillin and 10 mg/mL streptomycin in a 37° C humidified incubator containing 5% CO_2. Media containing 0.5 mg/mL G418 were used for maintenance of the transfected cell lines.

The recombinant pNSE-IRES2-EGFP-C1/CPXM2 plasmid and pNSE-IRES2-EGFP-C1 plasmid (negative control) were obtained from Nanjing KeyGen Biotech Co., Ltd. LX2 cells (1.2x105 cells/well) were plated into 6-well plates to obtain a 70% confluence after 24 h of culture. The aforementioned plasmids were transfected into LX2 cells using Lipofectamine® 2000 reagent (cat. no. 11668027, Invitrogen; Thermo Fisher Scientific, Inc.), and successfully transfected cells were selected using G418 (cat. no.108321-42-2, Sigma-Aldrich; Merck KGaA).

Reverse Transcription-Quantitative PCR (RT-qPCR)

The RT-qPCR assay was conducted as previously defined.[19] Total RNA was extracted from cell cultures using RNAiso Plus (cat. no. 9108, Takara Bio, Inc.) following the manufacturer's protocols and the expression level was investigated via the 2-ΔΔCq method.[20] The experiments were conducted 3 times in duplicate and GAPDH was taken as the internal control. The sequences of the primers were as follows: CPXM2 forward, 5′-GTHCCHCCGGGAAGAAATGAC -3′, and reverse, 5′-CCTCCCTTGAGTGATGACACC-3′; GAPDH forward, 5′-TGA AGGTCGGAGTCA ACGGA TTTGGT-3′, and reverse, 5′-CATGTGGGCCATGAGGT CCACCAC-3′ (synthesized by Takara Bio, Inc.).

Western Blotting

The total protein from cultured cells and liver tissues was isolated using RIPA lysis buffer containing 1% phenylmethanesulfonyl fluoride as previously defined.[21] The protein concentrations were investigated by a bicinchoninic acid (BCA) assay, and 10 μL protein was loaded into each well for sodium dodecylsulphate polyacrylamide gel electrophoresis (SDS-PAGE). Then, the separated proteins were electro-transferred to polyvinylidene fluoride (PVDF) membranes and blocked with 5% skimmed milk diluted in TBS-Tween 20 buffer (TBST) at room temperature (RT) for 2 h. Subsequently, the PVDF membranes were probed with primary antibodies against human gp130 (cat. no. 9145, Cell Signaling Technology, Inc), Stat1 (cat. no. 9139, Cell Signaling Technology, Inc), phospho- Stat1 (cat. no. 9167, Cell Signaling Technology, Inc), phospho-JAK2 (cat. no. 68790, Cell Signaling Technology, Inc), JAK2 (cat. no. 13531, Cell Signaling Technology, Inc), CPXM2 (cat. no. ab201077, Abcam, USA) or β-actin (cat. no. ab8226, Abcam, USA) at a dilution of 1:1000 at 4°C overnight. After washing 3 times with TBST, the PVDF membranes were probed with horseradish peroxidase (HRP) -conjugated secondary antibody (cat. no. sc-2357, Santa Cruz Biotechnology, Inc; 1:10,000) at RT for 2 h. Then, the bands were visualized via enhanced chemiluminescence (ECL) reagents (GE Healthcare Life Sciences) and evaluated with Image Lab version 6.0.1 (Bio-Rad Laboratories Inc.).

Immunofluorescence Assay

After washing 3 times with PBS, the cultured cells were fixed with 4% paraformaldehyde for 20 min. Subsequently, 0.5% Triton X-100 diluted in PBS was utilized to permeabilize the cells for 10 min, and the cells were blocked with 5% normal bovine serum in TBST for 30 min at 37°C. Then, the pretreated cells were incubated with the anti-CPXM antibody (cat. no. ab201077, Abcam, at 1:100) at 4°C overnight and probed with a PE-conjugated secondary antibody (cat. no. sc-3753, Santa Cruz Biotechnology, Inc; 1:1000) diluted in PBS for 1 h in the dark. The cell nuclei were stained with 0.1 μg/mL DAPI at RT for 5 min. The

probed cells were visualized and imaged by a fluorescence microscope (Olympus Corporation).

Cell Proliferation Assay

Stably transfected LX2 and Huh1 cells were plated in 96-well plates at 2x103 cells per well and cultured for 12, 24, 36, 48, 72 or 96 h. Then, 10 μL CCK8 reagent (cat no. C0038, Beyotime Institute of Biotechnology, Haimen, China) was supplemented to each well and further incubated with the cells at 37°C for 1 h. The absorbance at 496 nm for each well was detected by a microplate reader (BioTek China).

Colony Formation Assay

Briefly, cultured LX2 and Huh1 cells were plated in 6-well plates at a concentration of $5x10^2$ cells per well and maintained for 14 days in a 37°C incubator. Then, the formed colonies were washed with PBS 2 times for 5 min and fixed with methanol for 30 min. Then, the colonies were stained using 0.1% crystal violet diluted in PBS for 15 min. The formed cell colonies that contained more than 96 cells were counted.

Matrigel Invasion Assay

Briefly, the transfected LX2 and Huh1 cells ($4x10^5$ cells/mL) were seeded onto a membrane coated with Matrigel in the upper chamber of a 24-well Transwell insert. For cell movement, DMEM with 20% FBS was placed in the lower chamber. Then, the Transwell chamber was rinsed after incubation for 24 h at 37°C, and fixed in methanol, stained with 0.1% crystal violet (Beyotime Institute of Biotechnology), and the number of invaded cells per well was calculated in six randomly selected fields.

Wound Healing Assay

Briefly, transfected LX2 and Huh1 cells were cultured to ~100% confluence in 12-well plates. Mitomycin C (10 μg/mL) was used to pretreat the cells before scratching for 2 h to inhibit the proliferation of LX2 and Huh1 cells. A 20 μL pipette tip was utilized to create a scratch wound, and the scratch wound was imaged at the same position at 0, 12 and 24 h.

Short Hairpin RNA (shRNA) Assay

Four plasmids, pGCIL-gp130-shRNA, pGCIL-CPXM2-shRNA, pGCIL-scramble, and pGCIL-green fluorescent protein (GFP), the vesicular stomatitis virus G-protein (VSV-G) expression plasmid, and virion-packaging elements (pHelper 1.0) were purchased from Nanjing KeyGen Biotech Co., Ltd. 293T cells were cultured in a 6-well dish at 37°C for 24 h to achieve 70–80% confluence. Four plasmids namely, 10 μg pGCIL-gp130-shRNA or pGCIL-CPXM2-shRNA, and either 5 μg pGCIL-scramble, 5 μg pGCIL-GFP, 5 μg VSV-G expression plasmid and 5 μg pHelper 1.0 plasmid were added to media without FBS and mixed with 50 μL Lipofectamine® 2000 (cat. no. 11668027, Invitrogen; Thermo Fisher Scientific, Inc.) to an ultimate capacity of 1.0 mL. Subsequently, this mixture was supplemented with the cultured 293T cells. The cells were transfected with viral stocks as previously described,[22] and two clones of gp130-shRNA transfected cells were expanded and used in subsequent experiments.

Patients and Tissue Samples

The patients were enrolled between January 2006 and June 2013 and signed informed consent prior to the study. HCC sections were collected from 102 HCC patients from The First Hospital of Jilin University. The inclusion criteria were as follows: i) pathological diagnosis of HCC; ii) no evidence of secondary tumors or history of another cancer; iii) or history of chemotherapy or radiotherapy. The clinicopathological characteristics of HCC patients, such as age, sex, tumor-node-metastasis (TNM) and distant metastasis, are summarized in Table 1. Histological noncancerous hepatic sections were obtained from 100 hepatitis patients, including 60 men and 40 women admitted to The First Hospital of Jilin University between January 2008 and October 2014. The average age of the hepatitis patients was 64 years.

Immunohistochemistry (IHC)

Briefly, following deparaffinization, rehydration and antigen retrieval, the slides were blocked with 5% normal bovine serum in TBST for 30 min at 37°C, and the slides were incubated with the anti-CPXM2 antibody (1:296 dilution; cat. no. ab201077, Abcam, at 1:100) and anti-gp130 (1:396 dilution; cat. no. 9145, Cell Signaling Technology, Inc) overnight at 4°C. Normal rat immunoglobulin G (1:196 dilution; cat. no. D110964, Sangon Biotech Co. Ltd.) was used instead of the aforementioned primary antibodies for the negative control. Then, after washing with PBS, the slides were incubated with a horseradish peroxidase (HRP)-conjugated secondary antibody (1:5000; cat. no. A0192, Beyotime Institute of Biotechnology) at RT for 1 h. Subsequently, the slides were visualized using 3,3-diaminobenzidine (DAB; Gene Tech, Shanghai, China) and

Table 1 Expression of CPXM2 and the Clinicopathological Characteristics of Patients with HCC

Clinicopathological Characteristic	n	CPXM2 +	CPXM2 -	P-value
HCC tissue	102	72	30	<0.01[a]
Hepatic tissue	100	35	65	
Age, years				0.431*
≤60	71	53	18	
>60	31	19	12	
HbsAg				0.762*
+	85	63	22	
–	17	9	8	
Distant metastasis				<0.01[a]
+	71	59	12	
–	31	13	18	
Serum AFP, ng/mL				0.587*
<400	60	43	17	
>400	42	29	13	
TNM stage (AJCC)				0.009[a]*
I–II	62	39	23	
III–IV	40	33	7	

Notes: [a]P<0.01, *Not statistically significant as determined using a χ^2 Goodness-of-Fit Test.

Abbreviations: CPXM2, carboxypeptidase X, M14 family member 2; HCC, hepatocellular carcinoma; HbsAg, hepatitis B surface antigen; AFP, α fetoprotein; TNM, Tumor-Node-Metastasis; AJCC, American joint Committee on Cancer.

counterstained using hematoxylin (H&E; Gene Tech, Shanghai, China). CPXM2 expression was semi-quantitatively characterized as high or low on account of a modified H score system as previously described.[23]

Statistical Analysis

The data are presented as the mean ± SD and were analyzed using GraphPad Prism version 7 (GraphPad Software, Inc.) and SPSS version 22 (IBM Corp.). The Chi-squared test and one-way ANOVA with Tukey's post hoc tests were utilized to estimate the alterations between different groups. Statistical analyses and the difference in overall survival time were investigated using the Kaplan-Meier method and the Log rank test.

Results

CPXM2 Is Highly Expressed in HCC Cell Lines and Tissues

The comprehensive expression patterns of CPXM2 in human hepatic stellate cells and HCC cells were assayed. Data obtained from RT-qPCR and Western blotting displayed that the mRNA and protein expression levels of CPXM2 expression were lower in LX2 cells, and higher in the Hep3B, Huh1 and MHCC97H cell lines (Figure 1A–C).

Additionally, CPXM2 expression was measured in 102 HCC and 100 nonneoplastic hepatic tissues (Figure 1D). CPXM2 expression was determined to be high in 70.59% (71/102) of HCC tissues and 35.00% (35/100) of noncancerous hepatic tissues (Table 1). The correlations between CPXM2 levels and the clinical characteristics of patients with HCC were also determined, and CPXM2 expression was not distinctly related to clinical characters such as age (P=0.431), HBsAg infection (P=0.762), or serum α-fetoprotein (P=0.587), but it was correlated with TNM stage (P=0.009) and distant metastasis (P=0.001) in patients with HCC (Table 1). The changes in CPXM2 expression levels between nonneoplastic tissues and HCC tissues were also investigated. As displayed in Figure 1E and F, Western blotting analysis revealed a higher expression level of CPXM2 (P=0.005) in HCC tissues (102 cases) than in noncancerous hepatic tissues (100 cases). In addition, as illustrated in Figure 1G, a notably overall survival time was found in patients with a high expression level of CPXM2 (median survival, 34.76 months) versus patients with a low CPXM2 expression level (median survival, 46.34 months; P=0.0027).

Effect of CPXM2 on the Malignancy of Hepatic Stellate Cells

Hepatic stellate cells transfected with the pNSE-IRES2-EGFP-C1/CPXM2 plasmid or pNSE-IRES2-EGFP-C1 plasmid were termed LX2-CPXM2 or LX2-Vector, respectively. As displayed in Figure 2A and B, the CPXM2 protein was overexpressed (P=0.0001) in the LX2-CPXM2 group compared with the LX2-Vector group. Moreover, the phosphorylation levels of Stat1 (P=0.0001) and JAK2 (P=0.0032) were notably higher following CPXM2 overexpression (Figure 2A and B). Furthermore, immunofluorescence analysis showed that CPXM2 was localized to the cell cytoplasm (Figure 2C).

In addition, a CCK-8 assay was utilized to examine the proliferation of LX2 cells. As revealed in Figure 2D, the LX2-CPXM2 cells have a meaningfully higher proliferative rate than the empty vector cells (P=0.002). The data observed from the plate cloning assay suggested that the viability of LX2 cells was meaningfully enhanced after transfection with the CPXM2 overexpression plasmid (P=0.001; Figure 2E). Furthermore, the data obtained

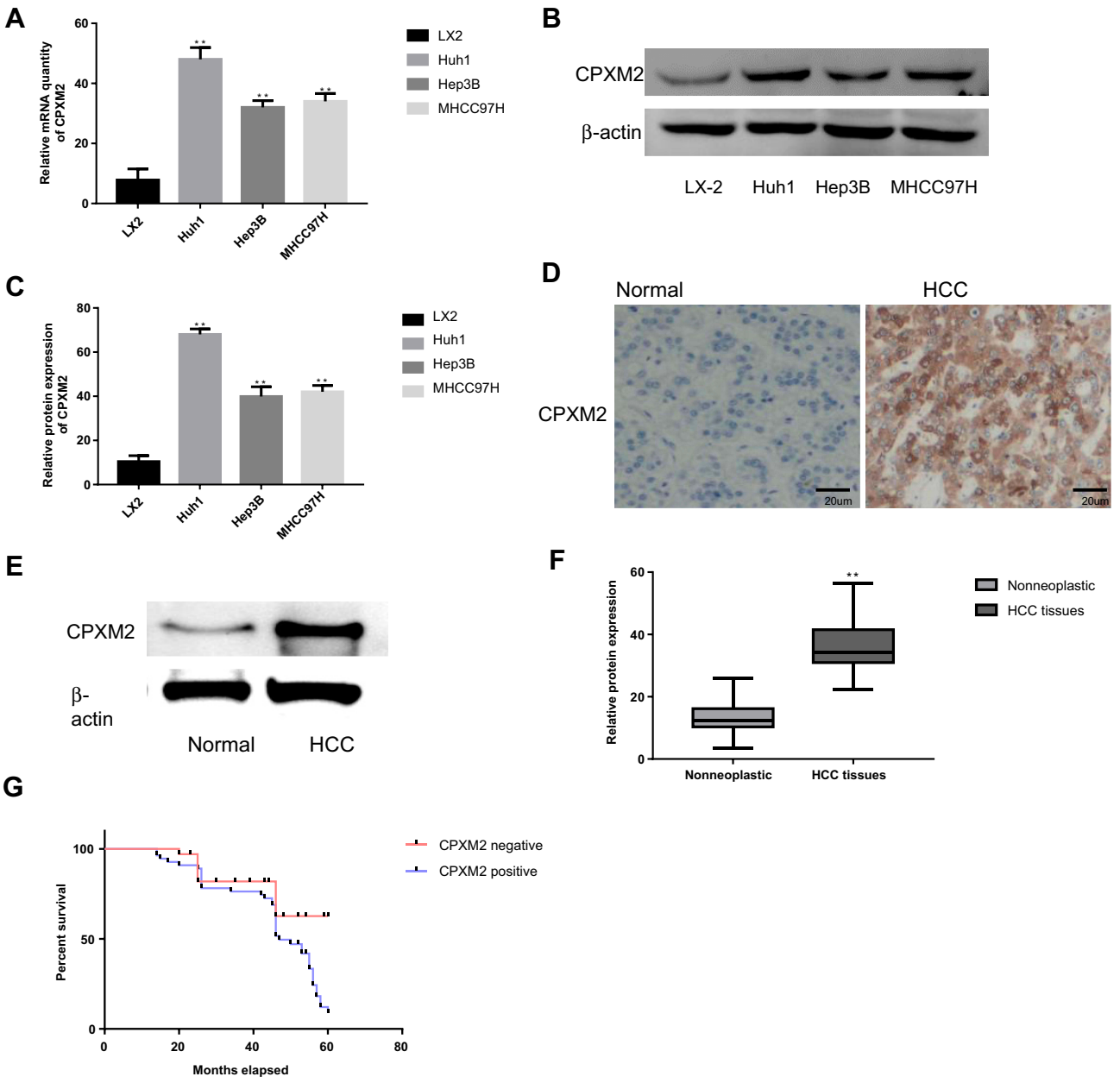

Figure 1 Expression levels of CPXM2 in. hepatocytes and HCC cells. (**A**) Relative mRNA expression levels of CPXM2 in HCC cell lines and a hepatic stellate cell line. **P<0.01 vs LX2. (**B**) Protein expression of CPXM2 in HCC cell lines and a stellate cell line. (**C**) Relative protein expression levels of CPXM2 in HCC cell lines and a hepatic stellate cell line. **P<0.01 vs LX2. (**D**) CPXM2 protein expression in HCC tissues. Scale bar, 20 μm. (**E**) Representative Western blot of CPXM2 protein expression in HCC tissues and hepatic tissues. (**F**) Relative protein expression level of CPXM2 in HCC tissues versus hepatic tissues. **P<0.01. (**G**) Association between CPXM2 expression and survival time in patients with HCC.

Abbreviations: HCC, hepatocellular carcinoma; CPXM2, carboxypeptidase X, M14 family member 2.

from a Matrigel invasion assay suggested that the invasion capacity was meaningfully increased in LX2 cells transfected with the CPXM2 overexpression plasmid (P=0.0001; Figure 2F). Similarly, evidence obtained from the wound-healing assay revealed that the migration was notably enhanced in the LX2-CPXM2 cells after 12 and 24 h verus the LX2-Vector group [P=0.0012 (12 h) and P=0.0032 (24 h); Figure 2G]. These data suggested that CPXM2 promoted the malignancy of hepatic stellate cells in vitro.

Effect of CPXM2 Knockdown on the Malignancy of HCC Cells

The expression level of CPXM2 and any changes in the phosphorylation status of members of the JAK2/Stat1

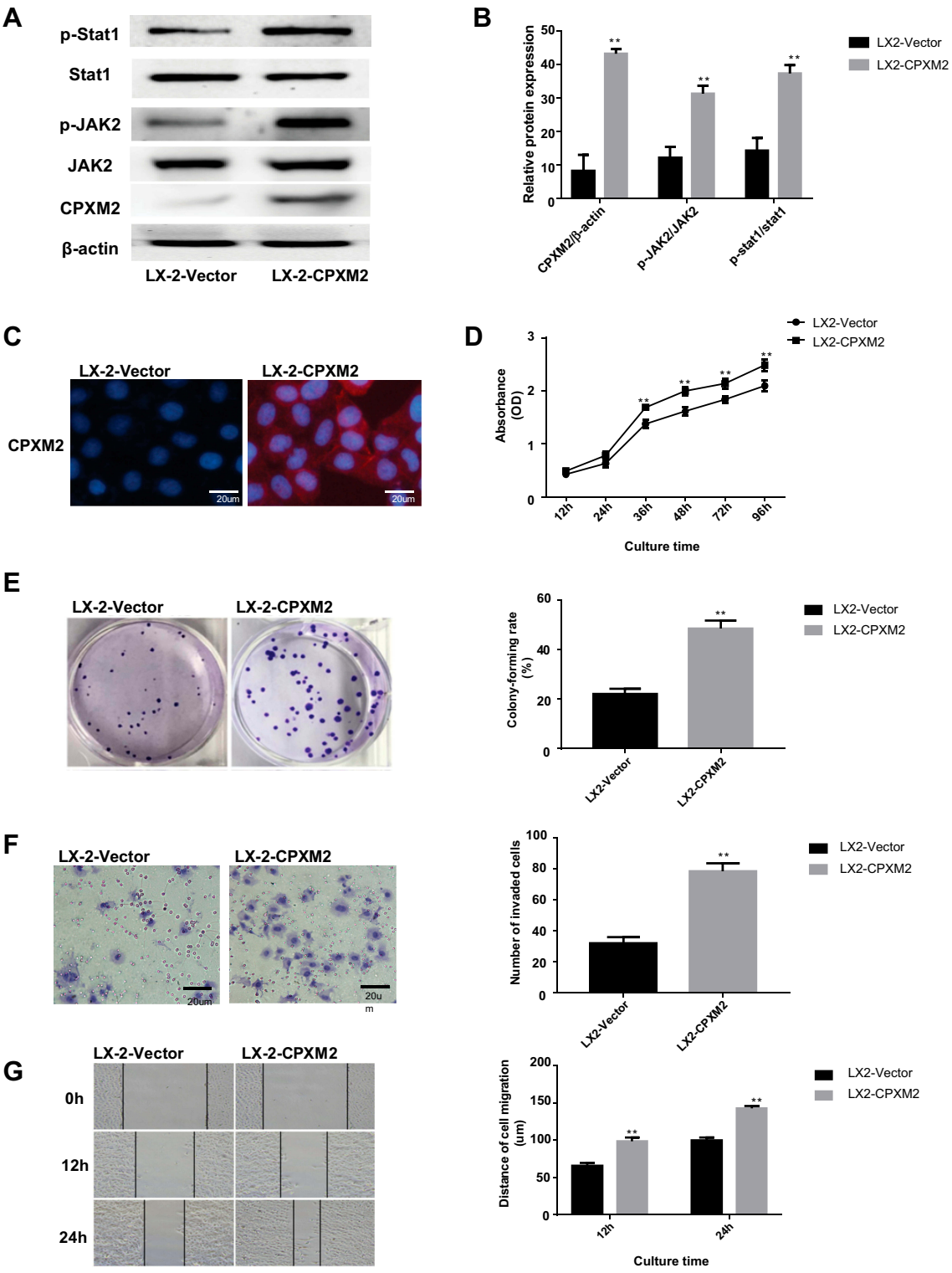

Figure 2 Effect of CPXM2 on the proliferation and metastasis of hepatic stellate cells in vitro. (**A**) Examination of the effect of CPXM2 on the phosphorylation levels of JAK2 and Stat1 in LX2 cells using Western blot analysis. (**B**) Relative protein expression level of CPXM2 and the phosphorylation status of JAK2 and Stat1 in LX2 cells. **P<0.01. (**C**) Examination of CPXM2 in LX2 cells using immunofluorescence. The CPXM2 protein was stained red (labeled with PE-conjugated secondary antibody), and the nucleus was stained blue (stained with DAPI). Scale bar, 20 μm. (**D**) Growth curves of LX2 cells transfected with a CPXM2 overexpression plasmid determined by Cell Counting Kit-8 assay. **P<0.01. (**E**) A plate colony formation assay was used to determine the effect of CPXM2 on the proliferative capacity of LX2 cells. **P<0.01. (**F**) Matrigel invasion assay was used to examine the effect of CPXM2 on the invasive capacity of LX2 cells in vitro (left), and corresponding statistical analysis of invasive cells (right). Scale bar, 20 μm; **P<0.01. (**G**) Wound-healing assay to detect the effect of CPXM2 on the migratory ability of LX2 cells in vitro (left), and the corresponding statistical analysis (right). **P<0.01.

Abbreviations: OD, optical density; CPXM2, carboxypeptidase X, M14 family member 2; Stat1, signal transducer and activator of transcription 1; JAK2, Janus kinase 2.

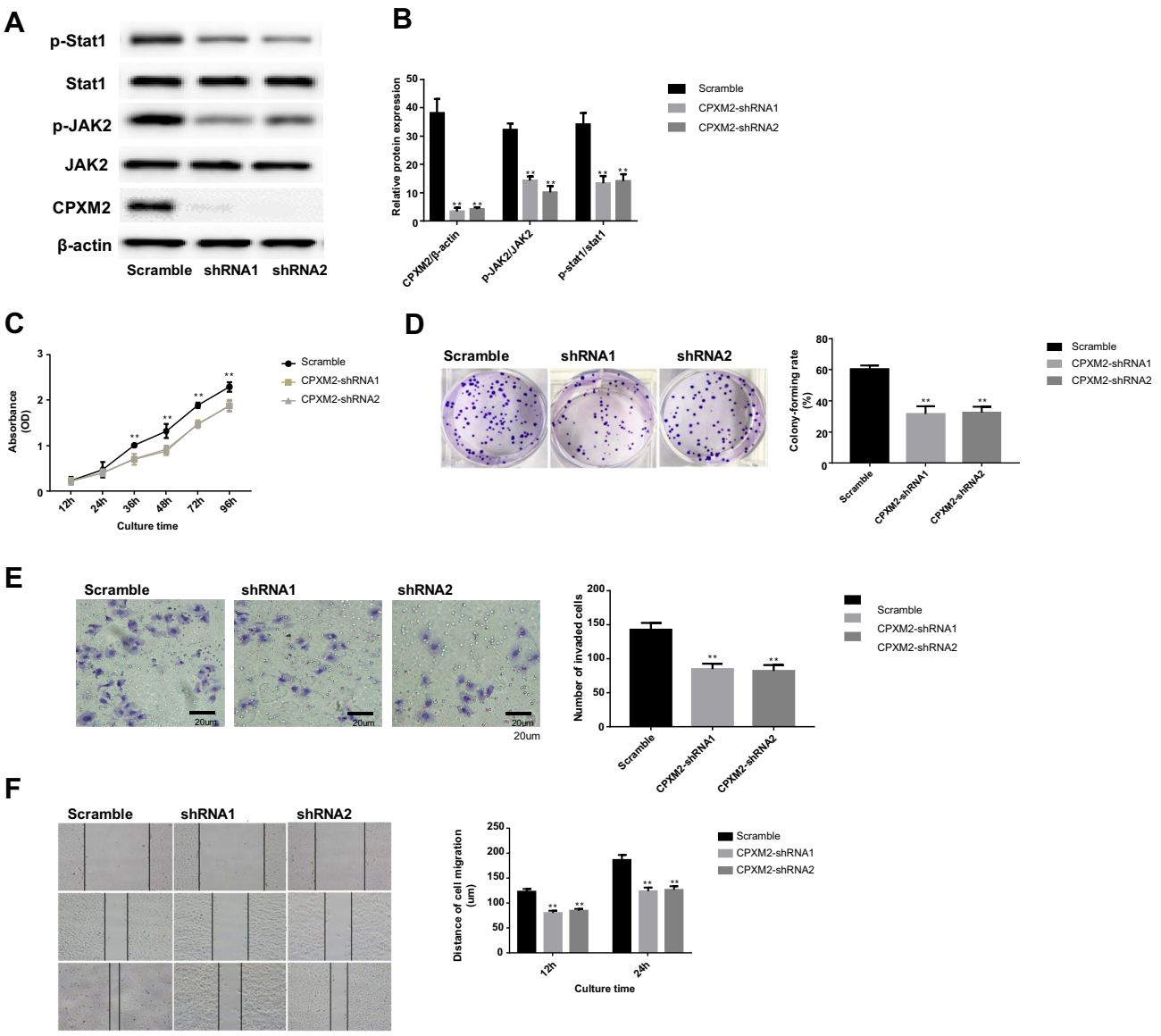

Figure 3 The effects of shRNA-mediated silencing of CPXM2 expression in HCC cells. (**A**) Western blotting was used to examine the effects of CPXM2 silencing and the activation of the JAK2/Stat1 signaling pathway in Huh1 cells. (**B**) Corresponding statistical analysis of the activation of the JAK2/Stat1 signaling pathway. **P<0.01 vs scramble. (**C**) Growth curves of Huh1 cells determined using a Cell Counting Kit-8 assay. **P<0.01 vs scramble. (**D**) A colony formation assay was used to explore the proliferative capacity of Huh1 cells. **P<0.01 vs scramble. (**E**) A Matrigel invasion assay to examine the impact of CPXM2 silencing on the invasive ability of Huh1 cells in vitro, and corresponding statistical analysis of the number of invading cells. Scale bar, 20 μm. **P<0.01 vs scramble. (**F**) Wound-healing assay to determine the migratory ability of Huh1 cells in vitro (left), and the corresponding statistical analysis (right). **P<0.01 vs scramble.

Abbreviations: shRNA, short hairpin RNA; HCC, hepatocellular carcinoma; CPXM2, carboxypeptidase X, M14 family member 2; Stat1, signal transducer and activator of transcription 1; JAK2, Janus kinase 2; p-, phosphorylated.

signaling pathway were assessed using Western blotting analysis (Figure 3A and B). The expression level of CPXM2 and the ratio of Stat1 and JAK2 phosphorylation were notably decreased in Huh1 cells (P=0.0014 and P=0.0007, respectively) following CPXM2 silencing.

Besides, the CCK-8 assay (Figure 3C) and plate cloning assay (Figure 3D) showed that the proliferative capacity (P=0.0021 and P=0.0015, respectively) and cell viability (P=0.0012 and P=0.0005, respectively) of Huh1 cells were notably decreased following CPXM2 silencing.

The evidence obtained from the Matrigel invasion and wound-healing assays (Figure 3E and F) showed that the invasive (P=0.0003 and P=0.0012, respectively) and migratory capabilities (P=0.0002 and P=0.0001, respectively) of cells transfected with CPXM2-shRNA were notably decreased.

gp130 Is Concurrently Expressed with CPXM2 in HCC Tissues

The expression of gp130 was determined in 102 HCC and 100 nonneoplastic hepatic tissues (Figure 4A). gp130 was highly expressed in 65.68% (67/102) of the HCC tissues and 29.00% (29/100) of the nonneoplastic hepatic tissues (Table 1). No correlation was found between gp130 expression and patient age (P=0.642), HBsAg infection (P=0.726), or serum α-fetoprotein (P=0.385). However, gp130 expression was related to distant metastasis (P=0.001) and TNM stage (P=0.014) in patients with HCC (Table 2). In addition, the protein expression level of gp130 was meaningfully higher in the 102 HCC tissues than in the 100 noncancerous hepatic tissues (P=0.0012; Figure 4B and C). Moreover, as illustrated in Figure 4D, a notably shorter overall survival time was found in patients with high levels of gp130 expression (median survival, 35.24 months) than in patients with low expression levels of gp130 (median survival, 48.67 months; P=0.0053). In addition, the correlations between gp130 and CPXM2 expression was also assessed. As shown in Table 3, gp130 and CPXM2 were concurrently expressed in HCC tissues and nonneoplastic mucosal tissues (P=0.0012; Table 3).

Impacts of gp130/JAK2/Stat1 on Malignancy in Hepatic Stellate Cells Overexpressing CPXM2

The impacts of the gp130/JAK2/Stat1 signaling pathway on the malignancy of hepatic stellate cells were investigated. As revealed in Figure 5A and B, the phosphorylation levels of JAK2 (P=0.0013 and P=0.0021, respectively) and Stat1 (P=0.0024 and P=0.0021, respectively) were notably decreased following knockdown of gp130 (P=0.0001) in LX2 cells overexpressing CPXM2.

As displayed in Figure 5C and D, the proliferation rate of LX2 cells overexpressing CPXM2 was notably decreased (P=0.0011 and P=0.0003, respectively) after gp130-shRNA transfection (Figure 5C and D). Furthermore, these observations implied that the quantity of invasive LX2-CPXM2 cells was notably decreased following transfection with gp130-shRNA (P=0.0013 and P=0.0021, respectively; Figure 5E). In addition, the migratory capacity of cells transfected with gp130-shRNA was notably decreased compared with that of the scrambled group after 12 h (P=0.0032 and P=0.0021, respectively; Figure 5F) and 24 h (P=0.0012 and P=0.0003, respectively; Figure 5F).

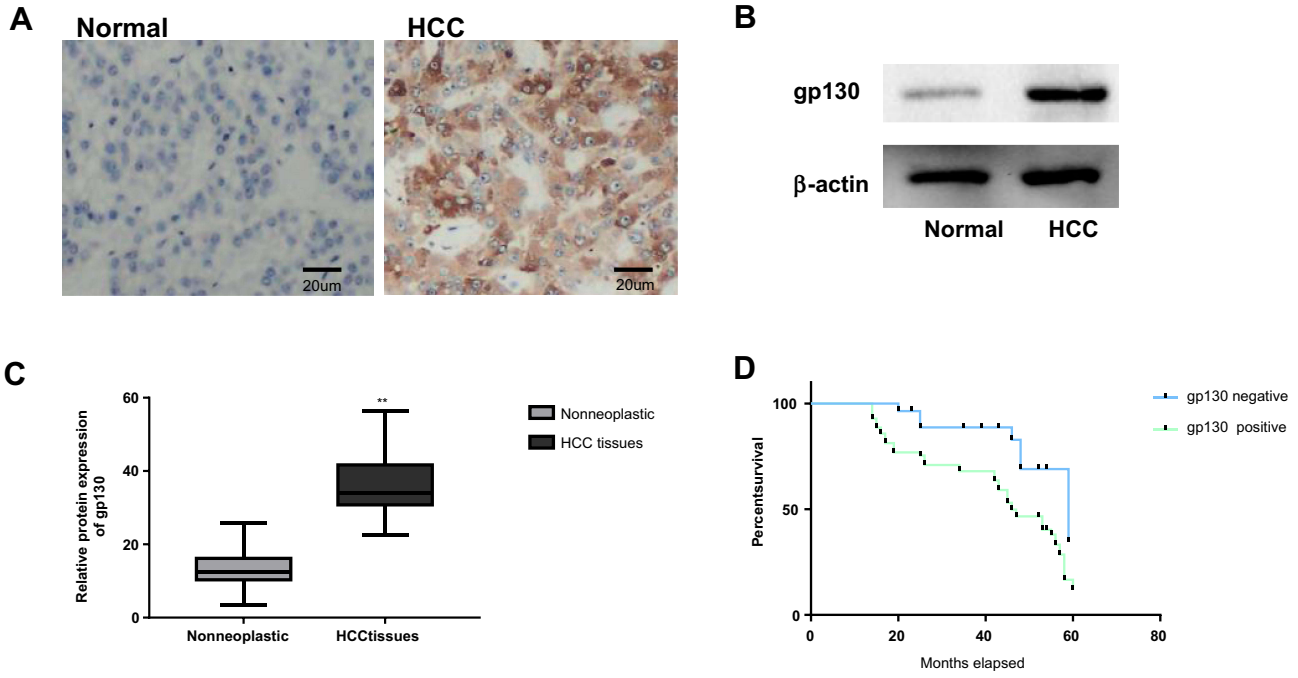

Figure 4 Expression levels of gp130 in hepatic tissues and HCC tissues. (**A**) Histopathological analysis of gp130 protein expression in hepatic tissues and HCC tissues. Scale bar, 20 μm. (**B**) Western blot of gp130 in HCC tissues compared with hepatic tissues. (**C**) Relative protein expression levels of gp130 in HCC tissues compared with hepatic tissues. **P<0.01. (**D**) Association between gp130 expression and survival times in patients with HCC.

Abbreviations: HCC, hepatocellular carcinoma; gp130, glycoprotein 130.

Table 2 Expression of gp130 and the Clinicopathological Characteristics of Patients with HCC

Clinicopathological Characteristic	n	gp130 +	gp130 –	P-value
HCC tissue	102	67	35	<0.01[a]
Hepatic tissue	100	29	71	
Age, years				0.642*
≤60	71	49	22	
>60	31	18	13	
HbsAg				0.726*
+	85	56	29	
–	17	11	6	
Distant metastasis				<0.01[a]
+	71	57	14	
–	31	10	21	
Serum AFP, ng/mL				0.385*
<400	60	40	20	
>400	42	27	15	
TNM stage				0.014*
I–II	61	42	19	
III–IV	41	25	16	
CPXM2				<0.01[a]
+	71	55	16	
–	31	12	19	

Notes: [a]P<0.01, *Not statistically significant as determined using a χ^2 Goodness-of-Fit Test.

Abbreviations: CPXM2, carboxypeptidase X, M14 family member 2; HCC, hepatocellular carcinoma; HbsAg, hepatitis B surface antigen; AFP, α fetoprotein; TNM, Tumor-Node-Metastasis; AJCC, American joint Committee on Cancer; gp130, glycoprotein 130.

Discussion

CPs are zinc-dependent enzymes that have been reported to be correlated with a range of physiological and biological processes, such as oncogenesis. For example, carboxypeptidase E (CPE) is suggested to be dysregulated and participate in the metastases of serval human malignancies,[13,24] highlighting the vital role of certain CPs in the regulation of malignant biological properties. To date, some CPs have been recognized as potential therapeutic and diagnostic biomarkers. For instance, a recent study revealed that carboxypeptidase A4 (CPA4) predicted a poor prognosis in breast cancer and was identified as a therapeutic target in triple-negative breast cancer (TNBC).[25] Similarly, CPA4 was also implied to be identified as a factor correlated with poor prognosis in liver cancer and gastric cancer.[26,27] In addition, the CPN was suggested to have a vital biological role in breast cancer and was a promising biomarker for the effective diagnosis and treatment of breast cancer.[28] To date, more than 20 CPs have been identified as potential biomarkers in various human malignancies. However, the underlying mechanisms by which these CPs modify oncogenesis and tumor progression still need to be further elucidated.

Table 3 Correlation Between the Expression of CPXM2 and gp130 in HCC Tissues

Item	CPXM2 High	CPXM2 Low	φ	P-value
gp130 high	48	19	0.869	<0.01
gp130 low	24	11		
Item	**CPXM2 high**	**CPXM2 low**	**φ**	**P**
gp130 high	48	19	0.869	<0.01
gp130 low	24	11		

Abbreviations: CPXM2, carboxypeptidase X, M14 family member 2; HCC, hepatocellular carcinoma; gp130, glycoprotein 130.

Previously, research concerned with CPXM2 highlighted its roles in mental diseases, developmental disorders, and neurodegenerative disorders.[14–17] Çetinkaya et al reported that CPXM2 is associated with gene ontology terms involved in extracellular matrix organization of connective tissues.[14] A recent study revealed that CPXM2 had a positive role in tumor progression and predicted a poor prognosis in gastric cancer.[29] However, the molecular mechanism of CPXM2 and its roles in the tumor progression of the common human malignancy HCC have not been reported. In our study, CPXM2 was acknowledged as a promising tumor biomarker for HCC. CPXM2 expression was high in HCC sections, and the overexpression of CPXM2 had a positive impact on the tumor progression of HCC cells. Moreover, the high expression level of CPXM2 in HCC patients was notably related to distant metastasis and predicted a poor prognosis. This evidence strongly implies that dysregulation of CPXM2 was reported to be a potential biomarker for the early diagnosis and prognosis of HCC patients. Moreover, alterations in the phosphorylation status of members of the JAK2/Stat1 signaling pathway were also explored. Additionally, it was demonstrated that CPXM2 may function by modulating the gp130/JAK2/Stat1 signaling pathway. As the gp130/JAK2/Stat1 signaling pathway has a vital impact on tumorigenesis and tumor progression in numerous human malignancies,[18] our data suggest that CPXM2 may play a positive factor in HCC progression via regulating gp130/JAK2/Stat1 signaling.

However, there are serval limitations in the present research. Firstly, the sample size was not large enough, and characterizing CPXM2 as a gene biomarker requires additional studies with larger and more varied cohorts. Besides, the detailed molecular mechanisms of intracellular

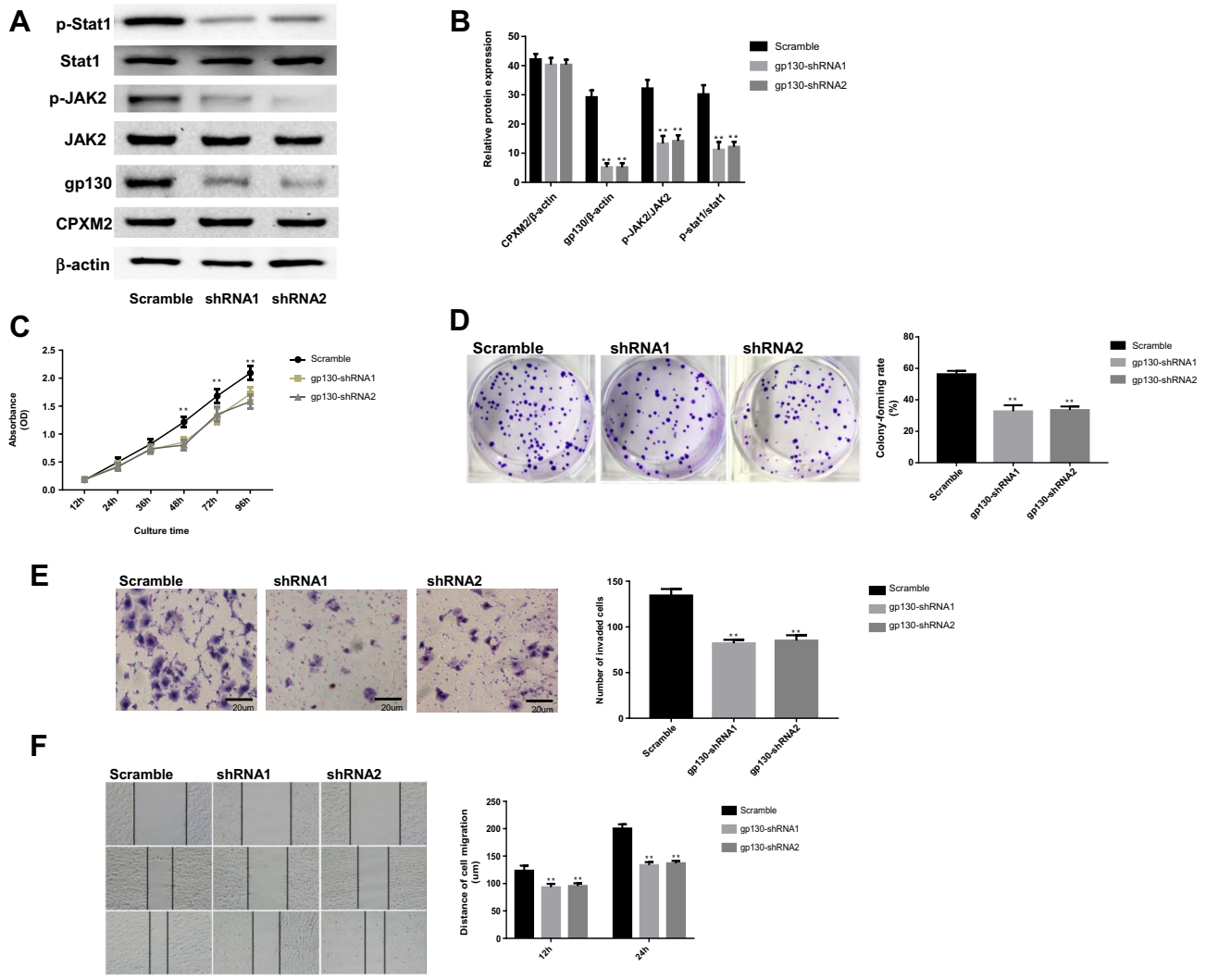

Figure 5 shRNA was used to silence gp130 expression in CPXM2-expressing LX2 cells. (**A**) Western blotting was used to examine the effects of gp130 silencing on the phosphorylation status of JAK2 and Stat1 in CPXM2-expressing LX2 cells. **P<0.01 vs scramble. (**B**) Quantitative analysis of JAK2/Stat1 phosphorylation levels. **P<0.01 vs scramble. (**C**) Growth curves of LX2 cells determined using a Cell Counting Kit-8 assay. **P<0.01 vs scramble. (**D**) A colony formation assay was used to determine the proliferative capacity of LX2 cells with gp130 silenced. **P<0.01 vs scramble. (**E**) A Matrigel invasion assay was used to examine the impact of gp130 silencing on the invasiveness of LX2 cells in vitro (left), and corresponding statistical analysis of the invasiveness cells (right). Scale bar, 20 μm. **P<0.01 vs scramble. (**F**) A wound-healing assay was used to examine the migratory ability of the LX2 cell line in vitro (left), and corresponding statistical analysis (right). **P<0.01 vs scramble.

Abbreviations: shRNA, short hairpin RNA; Stat1, signal transducer and activator of transcription 1; JAK2, Janus kinase 2; p-, phosphorylated; gp130, glycoprotein 130; CPXM2, carboxypeptidase X, M14 family member 2.

signal transduction from CPXM2 to JAK2 remain to be elucidated.

Conclusions

At present, the impacts and detailed mechanism of CPXMs in HCC remain unknown. Our study implies that CPXM2 is an active factor in HCC progression, and notably enhances the invasiveness and migration of HCC cells. A preliminary exploration of the detailed mechanism of this function was also conducted, and our data observed that CPXM2 impacts metastatic capacity via the gp130/JAK2/Stat1 signaling pathway in HCC.

Abbreviations

CPXM2, Carboxypeptidase X, M14 family member 2; JAK2, tyrosine kinase 2; HCC, hepatocellular carcinoma; AJCC, American Joint Committee on Cancer; Stat1, signal transducer and activator of transcription 1.

Ethics Approval and Informed Consent

All procedures in the present research concerning with human participants were in line with the ethical standards of the institutional and/or national research committee and

the 9864 Helsinki Declaration. Our study was approved by the Ethics Committee of Jilin University (approval no. JLU10012).

Consent for Publication

Written informed consent for publication was obtained. A copy of the consent form is available for review by the editor of this journal.

Data Sharing Statement

The datasets used and/or analyzed during the present study are available from the corresponding author on reasonable request.

Disclosure

The authors declare that they have no competing interests.

References

1. Mak LY, Cruz-ramon V, Chinchilla-lopez P, et al. Global epidemiology, prevention, and management of hepatocellular carcinoma. *Am Soc Clin Oncol*. 2018;38:262–279. doi:10.1200/EDBK_200939
2. Zhang G, Li R, Deng Y, Zhao L. Conditional survival of patients with hepatocellular carcinoma: results from the surveillance, epidemiology, and end results registry. *Expert Rev Gastroenterol Hepatol*. 2018;12(5):515–523. doi:10.1080/17474124.2018.1453806
3. Kulik L, El-serag HB. Epidemiology and management of hepatocellular carcinoma. *Gastroenterology*. 2019;156(2):477–491 e471. doi:10.1053/j.gastro.2018.08.065
4. Kamarajah SK, Frankel TL, Sonnenday C, Cho CS, Nathan H. Critical evaluation of the American Joint Commission on Cancer (AJCC) 8th edition staging system for patients with hepatocellular carcinoma (HCC): a Surveillance, Epidemiology, End Results (SEER) analysis. *J Surg Oncol*. 2018;117(4):644–650. doi:10.1002/jso.24908
5. Fu J, Li L, Yang XQ. Specificity of carboxypeptidases from actinomucor elegans and their debittering effect on soybean protein hydrolysates. *Appl Biochem Biotechnol*. 2011;165(5–6):1201–1210. doi:10.1007/s12010-011-9338-4
6. Zhang H, Yao Y, Yang H, et al. Molecular dynamics and free energy studies on the carboxypeptidases complexed with peptide/small molecular inhibitor: mechanism for drug resistance. *Insect Biochem Mol Biol*. 2012;42(8):583–595. doi:10.1016/j.ibmb.2012.04.005
7. Mallick S, Das J, Verma J, Mathew S, Maiti TK, Ghosh AS. Role of Escherichia coli endopeptidases and DD-carboxypeptidases in infection and regulation of innate immune response. *Microbes Infect*. 2019;21(10):464–474. doi:10.1016/j.micinf.2019.04.007
8. Song Y, Wang Q, Wang D, et al. Label-free quantitative proteomics unravels carboxypeptidases as the novel biomarker in pancreatic ductal adenocarcinoma. *Transl Oncol*. 2018;11(3):691–699. doi:10.1016/j.tranon.2018.03.005
9. Reytor Gonzalez ML, Alonso-Del-Rivero Antigua M, Hedstrom L, Kuzmic P, Pires JR. Sabellastarte magnifica carboxypeptidase Inhibitor: the first Kunitz inhibitor simultaneously interacting with carboxypeptidases and serine proteases. *Biochimie*. 2018;150:37–47. doi:10.1016/j.biochi.2018.04.024
10. Petrera A, Lai ZW, Schilling O. Carboxyterminal protein processing in health and disease: key actors and emerging technologies. *J Proteome Res*. 2014;13(11):4497–4504. doi:10.1021/pr5005746
11. Ferreira C, Rebola KG, Cardoso C, Bragatto I, Ribeiro AF, Terra WR. Insect midgut carboxypeptidases with emphasis on S10 hemipteran and M14 lepidopteran carboxypeptidases. *Insect Mol Biol*. 2015;24(2):222–239. doi:10.1111/imb.v24.2
12. Sapio MR, Fricker LD. Carboxypeptidases in disease: insights from peptidomic studies. *Proteonomics Clin Appl*. 2014;8(5–6):327–337. doi:10.1002/prca.201300090
13. Denis CJ, Lambeir AM. The potential of carboxypeptidase M as a therapeutic target in cancer. *Expert Opin Ther Targets*. 2013;17(3):265–279. doi:10.1517/14728222.2012.741122
14. Cetinkaya A, Taskiran E, Soyer T, et al. Dermal fibroblast transcriptome indicates contribution of WNT signaling pathways in the pathogenesis of Apert syndrome. *Turk J Pediatr*. 2017;59(6):619–624. doi:10.24953/turkjped.2017.06.001
15. Sabri A, Lai D, D'silva A, et al. Differential placental gene expression in term pregnancies affected by fetal growth restriction and macrosomia. *Fetal Diagn Ther*. 2014;36(2):173–180. doi:10.1159/000360535
16. Chen YC, Hsiao CJ, Jung CC, et al. Performance metrics for selecting single nucleotide polymorphisms in late-onset alzheimer's disease. *Sci Rep*. 2016;6:36155. doi:10.1038/srep36155
17. Hashimoto R, Ikeda M, Ohi K, et al. Genome-wide association study of cognitive decline in schizophrenia. *Am J Psychiatry*. 2013;170(6):683–684. doi:10.1176/appi.ajp.2013.12091228
18. Rebouissou S, Amessou M, Couchy G, et al. Frequent in-frame somatic deletions activate gp130 in inflammatory hepatocellular tumours. *Nature*. 2009;457(7226):200. doi:10.1038/nature07475
19. Zhang X, Wang X, Wang A, Li Q, Zhou M, Li T. CLDN10 promotes a malignant phenotype of osteosarcoma cells via JAK1/Stat1 signaling. *J Cell Commun Signal*. 2019;13(3):395–405. doi:10.1007/s12079-019-00509-7
20. Zhao S, Zhou L, Niu G, Li Y, Zhao D, Zeng H. Differential regulation of orphan nuclear receptor TR3 transcript variants by novel vascular growth factor signaling pathways. *FASEB J*. 2014;28(10):4524–4533. doi:10.1096/fsb2.v28.10
21. Zhang X, Wang H, Li Q, Li T. CLDN2 inhibits the metastasis of osteosarcoma cells via down-regulating the afadin/ERK signaling pathway. *Cancer Cell Int*. 2018;18:160. doi:10.1186/s12935-018-0662-4
22. Wang P, Yu B, Wang C, Zhou S. C-terminal of E1A binding protein 2 promotes the malignancy of osteosarcoma cells via JAK1/Stat3 signaling. *J Cell Commun Signal*. 2019. doi:10.1007/s12079-019-00523-9
23. Yang Y, Yang H, McNutt MA, et al. LAPTM4B overexpression is an independent prognostic marker in ovarian carcinoma. *Oncol Rep*. 2008;20(5):1077–1083.
24. Cawley NX, Wetsel WC, Murthy SR, Park JJ, Pacak K, Loh YP. New roles of carboxypeptidase E in endocrine and neural function and cancer. *Endocr Rev*. 2012;33(2):216–253.
25. Handa T, Katayama A, Yokobori T, et al. Carboxypeptidase A4 accumulation is associated with an aggressive phenotype and poor prognosis in triple-negative breast cancer. *Int J Oncol*. 2019;54(3):833–844. doi:10.3892/ijo.2019.4675
26. Sun L, Guo C, Burnett J, et al. Association between expression of Carboxypeptidase 4 and stem cell markers and their clinical significance in liver cancer development. *J Cancer*. 2017;8(1):111. doi:10.7150/jca.17060
27. Sun L, Guo C, Yuan H, et al. Overexpression of carboxypeptidase A4 (CPA4) is associated with poor prognosis in patients with gastric cancer. *Am J Transl Res*. 2016;8(11):5071.
28. Cui R, Zhang P, Li Y. Role of carboxypeptidase N invasion and migration in breast cancer. *Anticancer Agents Med Chem*. 2016;16(9):1198–1202.
29. Niu G, Yang Y, Ren J, et al. Overexpression of CPXM2 predicts an unfavorable prognosis and promotes the proliferation and migration of gastric cancer. *Oncol Rep*. 2019;42(4):1283–1294. doi:10.3892/or.2019.7254